

# The dynamics of domain wall Skyrmions

Paul Jennings and Paul Sutcliffe

*Department of Mathematical Sciences, Durham University, Durham DH1 3LE, U.K.*

Email: paul.jennings@durham.ac.uk & p.m.sutcliffe@durham.ac.uk

May 2013

## **Abstract**

It has recently been shown that Skyrmions with a fixed size can exist in theories without a Skyrme term, providing the Skyrmion is located on a domain wall. Here we numerically compute domain wall Skyrmions of this type, in a (2+1)-dimensional  $O(3)$  sigma model with a potential term. Moreover, we investigate Skyrmion dynamics, to study both Skyrmion stability and the scattering of multi-Skyrmions. We demonstrate that scattering events in which both Skyrmions remain on the same domain wall are effectively one-dimensional, and at low speeds are well-approximated by kink scattering in the integrable sine-Gordon model. However, more exotic fully two-dimensional scatterings are also presented, in which Skyrmions that are initially on different domain walls emerge on the same domain wall.

# 1 Introduction

Skyrmions [1] are topological solitons in generalized sigma models that include a term in the Lagrangian that is quartic in the derivatives of the field. The role of this quartic Skyrme term is to provide a fixed finite size for the Skyrmion, as revealed by Derrick's theorem [2]. The original Skyrme model is a relativistic theory in (3+1)-dimensions, where Skyrmions describe baryons within an effective field theory. There is also a (2+1)-dimensional analogue of this theory, known as the baby Skyrme model [3]. This is a generalization of the  $O(3)$  sigma model, and has proved to be a useful testing ground for the study of several aspects of Skyrmions.

Non-relativistic cousins of the baby Skyrme model are also of interest in their own right. For example, Skyrmions play a role in the fractional quantum Hall effect [4] and have recently been experimentally observed in chiral magnets [5]. The Skyrme term is not appropriate for the description of these condensed matter systems and its role is replaced by other terms that may appear in a non-relativistic theory. In the case of quantum Hall ferromagnets its replacement is a non-local Coulomb interaction, and in chiral magnets it is the Dzyaloshinskii-Moriya interaction. For a review of Skyrmions and their varied applications see [6, 7].

It has recently been observed [8, 9] that static Skyrmions can exist in relativistic theories without a Skyrme term, providing the Skyrmion is located on a domain wall. In such a theory there is no replacement for the Skyrme term, but rather the finite fixed size of the Skyrmion derives from the presence of the domain wall. As theories containing higher derivative Skyrme terms can often be difficult to motivate physically, the presence of Skyrmions without the need for such a term opens up a new range of possibilities. In particular, domain walls in relativistic theories are studied in both cosmology and high energy physics, in contexts such as braneworld models and supersymmetric theories, where domain walls are important configurations that preserve a fraction of the supersymmetry. The results of this paper may therefore find applications in these fields. Furthermore, in the investigation of static Skyrmions, the type of dynamics plays no role, so applications to non-relativistic systems in condensed matter physics are also possible.

To date, studies of Skyrmions in relativistic theories without a Skyrme term have been restricted to the numerical construction of a static single Skyrmion on a domain wall in (2+1)-dimensions [9]. The form of the Skyrmion is quite different to that familiar from theories with a Skyrme term, so it is of interest to see what new phenomena appear. In this paper we present the first numerical investigations of Skyrmion dynamics and multi-Skyrmions in a (2+1)-dimensional theory of this type. We provide evidence for the stability of a Skyrmion and obtain some novel results on Skyrmion scattering. Although our study is concerned with a planar theory, we expect similar results to apply in (3+1)-dimensions.

## 2 The model and its static Skyrmion

The theory of interest in this paper is a relativistic (2+1)-dimensional O(3) sigma model with a potential term. It is given by the following Lagrangian density

$$\mathcal{L} = \frac{1}{2} \partial_\mu \mathbf{n} \cdot \partial^\mu \mathbf{n} - \frac{m^2}{2} (n_1^2 + n_2^2) + \frac{gm^2}{2} (n_1^2 + n_2^2)^2 n_2, \quad (2.1)$$

where  $\mathbf{n} = (n_1, n_2, n_3)$  is a unit vector and  $x_\mu$  are the spacetime coordinates with  $x_0 = t$ ,  $x_1 = x$  and  $x_2 = y$ . Here  $m > 0$  and  $0 < g < 1$  are parameters of the theory. This particular model has been chosen as the simplest example of a theory that has the required properties to support a domain wall Skyrmion. The essential features of the theory will become apparent below, but they are not very restrictive, so similar results should hold in a wide range of models.

The energy corresponding to (2.1) is

$$E = \int \left\{ \frac{1}{2} \partial_i \mathbf{n} \cdot \partial_i \mathbf{n} + \frac{1}{2} \partial_i \mathbf{n} \cdot \partial_i \mathbf{n} + \frac{m^2}{2} (n_1^2 + n_2^2) - \frac{gm^2}{2} (n_1^2 + n_2^2)^2 n_2 \right\} d^2x \quad (2.2)$$

where latin indices run over only the spatial components. The constraint  $0 < g < 1$  ensures that the energy density is non-negative. The potential term breaks the O(3) symmetry of the sigma model so that only the discrete symmetries  $n_1 \mapsto -n_1$  and  $n_3 \mapsto -n_3$  remain.

There are two vacuum solutions  $\mathbf{n} = (0, 0, \pm 1)$  and the energy vanishes for each of these. One of the motivations for our choice of the potential term is that the two vacuum fields remain the same antipodal points on the target sphere for all values of the parameters  $m > 0$  and  $g \in (0, 1)$ . This is not essential, and indeed in previous studies [8, 9] only linear and quadratic terms appear in the potential, with the result that the vacuum fields vary with the parameters of the theory and are not antipodal. The fact that our theory has fixed antipodal vacuum fields will simplify the description of the winding structure of the Skyrmion, so is simply for convenience.

A field with finite energy must tend to the same vacuum solution at spatial infinity, say  $\mathbf{n} \rightarrow (0, 0, 1)$  as  $x^2 + y^2 \rightarrow \infty$ . An application of Derrick's theorem [2] to the energy (2.2) quickly reveals that the only finite energy static solution is the trivial solution where  $\mathbf{n} = (0, 0, 1)$  at all points in the plane.

The conventional approach to allow Skyrmion solutions in this kind of theory is to introduce a Skyrme term into the Lagrangian density (2.1), which takes the form [1, 10]

$$\mathcal{L}_{Skyrme} = -(\partial_\mu \mathbf{n} \times \partial_\nu \mathbf{n}) \cdot (\partial^\mu \mathbf{n} \times \partial^\nu \mathbf{n}). \quad (2.3)$$

Skyrmion solutions have been computed in such theories with various potential terms, including the one given above with  $g = 0$  [11]. These Skyrmion solutions are classified by the integer-valued winding number

$$B = -\frac{1}{4\pi} \int \mathbf{n} \cdot (\partial_x \mathbf{n} \times \partial_y \mathbf{n}) d^2x \quad (2.4)$$

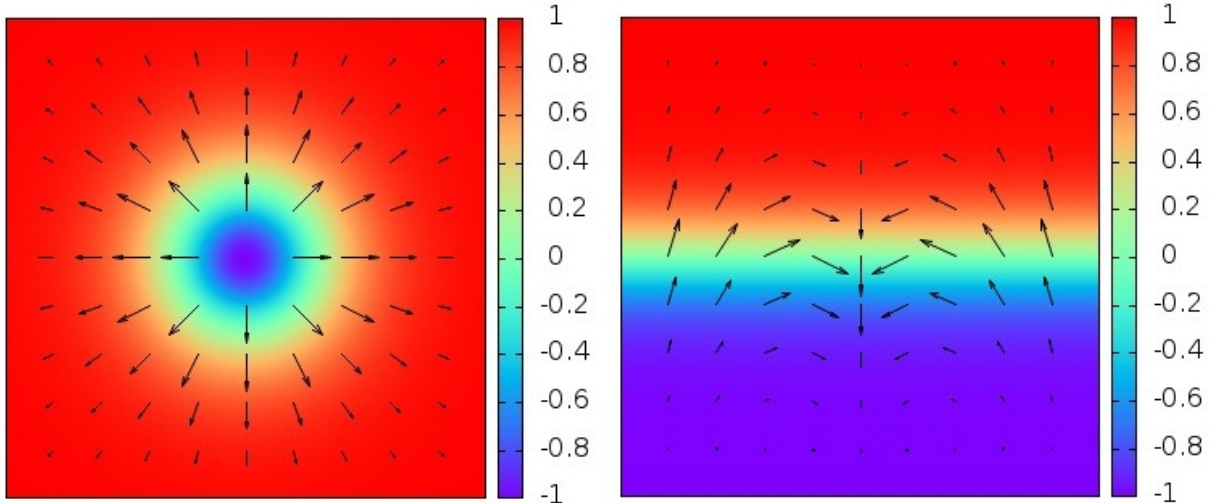


Figure 1: The winding structure in the  $(x, y)$  plane of a standard Skyrmion (left image) and a Skyrmion on a domain wall (right image). The colour represents the value of  $n_3$  and the arrow indicates the length and direction of the two-component vector  $(n_1, n_2)$ .

that counts the number of times that the field covers the target two-sphere,  $\mathbf{n} \cdot \mathbf{n} = 1$ , as  $(x, y)$  varies over the plane. By definition, the topological charge  $B$  is the number of Skyrmons in any given field configuration.

In the presence of a Skyrme term, the way in which the winding is realized for the standard single Skyrmion ( $B = 1$ ) is depicted in the left image in Figure 1. The colour indicates the value of  $n_3$ , which varies from the vacuum value  $n_3 = -1$  at the centre of the Skyrmion (chosen as the origin of the plane) to the vacuum value  $n_3 = 1$  at spatial infinity. The arrow represents the two-component vector  $(n_1, n_2)$ , from which it can be seen that on the circle  $x^2 + y^2 = a^2$ , with  $a$  positive and finite, this vector has a constant magnitude and takes all possible directions. This makes it clear that every point on the target sphere is obtained. The representative image shown is for the simplest case when  $g = 0$ , where the model has a global  $O(2)$  symmetry and the Skyrmion is axially symmetric, but the basic features of the winding structure remain the same for  $g > 0$ , even though the axial symmetry is broken. Shortly, we shall compare this standard realization of the winding structure with the form that it takes in the theory without a Skyrme term, where the Skyrmion is located on a domain wall.

The field equations that follow from (2.1) possess a static domain wall solution that is independent of  $x$  and interpolates between the two vacua. Explicitly, consider a solution of the form

$$\mathbf{n} = (0, \sin \theta, \cos \theta), \quad (2.5)$$

with  $\theta(y)$  satisfying the boundary conditions that  $\theta \rightarrow \pi$  as  $y \rightarrow -\infty$  and  $\theta \rightarrow 0$  as  $y \rightarrow \infty$ . These boundary conditions ensure that the domain wall interpolates between the vacua since  $\mathbf{n} \rightarrow (0, 0, \pm 1)$  as  $y \rightarrow \pm\infty$ . The position of the domain wall is an arbitrary parameter, which

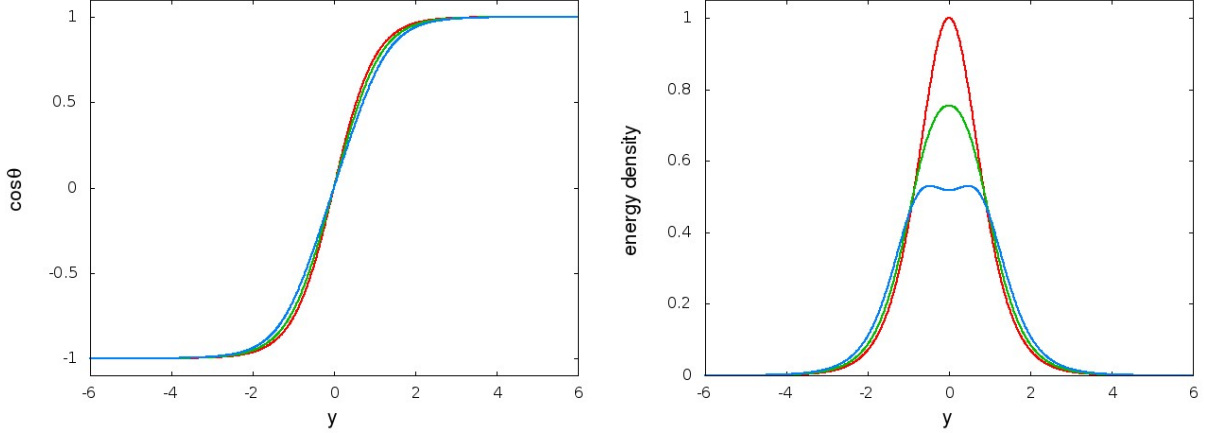


Figure 2: The left image is the field  $\cos\theta$  of the wall and the right image is the energy density. Plots for three values of the parameter  $g$  are shown:  $g = 0$  (red curves),  $g = 0.25$  (green curves);  $g = 0.5$  (blue curves).

we choose to fix by setting  $\theta(0) = \pi/2$ , so that the domain wall lies along the  $x$ -axis.

As the domain wall is independent of  $x$  then its energy is infinite. However, it has a finite tension (energy per unit length) given by

$$\mu = \int \left\{ \frac{1}{2}\theta'^2 + \frac{m^2}{2}(\sin^2\theta - g\sin^5\theta) \right\} dy. \quad (2.6)$$

The variation of this tension yields the equation satisfied by the static domain wall profile

$$\theta'' - m^2 \cos\theta \sin\theta \left(1 - \frac{5}{2}g\sin^3\theta\right) = 0. \quad (2.7)$$

If  $g = 0$  then the domain wall solution has the simple expression  $n_3 = \cos\theta = \tanh(my)$ , with tension  $\mu = 2m$ . For  $g > 0$  the domain wall equation is hyperelliptic and does not have an elementary explicit solution. However, it is a simple matter to obtain the domain wall solution numerically. In Figure 2 we plot the domain wall field  $\cos\theta$  (left image) and the energy density (the integrand in (2.6)) for three different values of the parameter  $g$ . We see that the field does not appear to be very sensitive to the value of  $g$  although there is a more significant change in the corresponding energy density.

Given a domain wall we may dress this configuration by imposing a winding of the  $(n_1, n_2)$  components along the domain wall. As we shall see, this produces a domain wall Skyrmion. Ignoring the back-reaction on the domain wall, we can use the domain wall field  $\theta(y)$  to obtain an effective (1+1)-dimensional theory for the Skyrmion dynamics along the wall. Explicitly, we assume  $\varphi(x, t)$  and consider a field of the form

$$\mathbf{n} = (\sin\varphi \sin\theta, \cos\varphi \sin\theta, \cos\theta). \quad (2.8)$$

If we restrict to the domain wall ( $y = 0$ ), where  $\theta = \pi/2$ , and substitute (2.8) into the Lagrangian density (2.1) the result is

$$\mathcal{L}_{SG} = \frac{1}{2}(\partial_t\varphi)^2 - \frac{1}{2}(\partial_x\varphi)^2 + \frac{gm^2}{2}\cos\varphi - \frac{m^2}{2}, \quad (2.9)$$

which is the Lagrangian density of the (1+1)-dimensional integrable sine-Gordon model (up to the addition of an irrelevant constant). The vacua of this theory are given by  $\varphi$  an integer multiple of  $2\pi$ , corresponding to the fact that along the domain wall ( $y = 0$ ) where  $n_3 = 0$ , we have that  $\mathbf{n} \rightarrow (0, 1, 0)$  as  $x \rightarrow \pm\infty$ . Given vacuum boundary conditions,  $\varphi \rightarrow 2\pi N_{\pm}$  as  $x \rightarrow \pm\infty$ , there is a conserved kink number  $N = N_+ - N_-$ . The static sine-Gordon kink with  $N = 1$  is given by

$$\varphi = 4 \tan^{-1} e^{m\sqrt{\frac{g}{2}}x}, \quad (2.10)$$

where we have positioned the kink at the origin.

Rather than restricting the Lagrangian density to the domain wall, an alternative method to derive an effective (1+1)-dimensional theory is to integrate over the spatial dimension perpendicular to the wall. This also produces a sine-Gordon theory, though with a slightly different scale, with the parameters in the sine-Gordon Lagrangian given by integrals involving the wall profile function  $\theta(y)$ . This approach is not as tractable as simply restricting to the wall, because of the lack of a simple explicit expression for  $\theta(y)$ . However, we have numerically obtained these parameters and compared the two effective theories. They are similar, but it turns out that the first approach yields a slightly better approximation to the full theory, as described later.

Using the kink function (2.10) in the field (2.8) gives a planar field configuration that describes a kink on a domain wall. Although this is not a static solution, we shall see that there is a static solution that is close to this field configuration. It is easy to verify that this field has Skyrmion number  $B = 1$ , where  $B$  is given by the integral expression (2.4).

The way in which the unit winding around the sphere is realized is depicted in the right image in Figure 1. Along lines parallel to the  $y$ -axis,  $n_3$  increases monotonically from  $-1$  to  $+1$ , and the vector  $(n_1, n_2)$  has a constant direction. Along lines parallel to the  $x$ -axis,  $n_3$  is constant and hence the vector  $(n_1, n_2)$  has constant magnitude, but rotates through one revolution, being asymptotically vertical at both ends of the line. It is again clear that every point on the target sphere is realized, although the structure of the winding is quite different to that of the standard Skyrmion. The location of the Skyrmion has the natural definition as the point in space at which the field takes the value  $(0, -1, 0)$ . This agrees with the position of the kink on the domain wall.

To obtain the true static Skyrmion we take the field (2.8) as an initial condition for a gradient flow energy minimization algorithm using the static version of the energy (2.2). The mixed boundary condition has the Dirichlet component  $\mathbf{n} \rightarrow (0, 0, \pm 1)$  as  $y \rightarrow \pm\infty$ , and the Neumann component  $\partial_x\mathbf{n} \rightarrow 0$  as  $x \rightarrow \pm\infty$ . The constant  $m$  in the theory (2.1) simply determines an overall scale and may be set to unity without loss of generality. For the numerical simulations presented in this paper we fix the generic parameter value  $g = \frac{1}{2}$ .



Figure 3: The energy density (left image) and the topological charge density (right image) of the static Skyrmion on a domain wall.

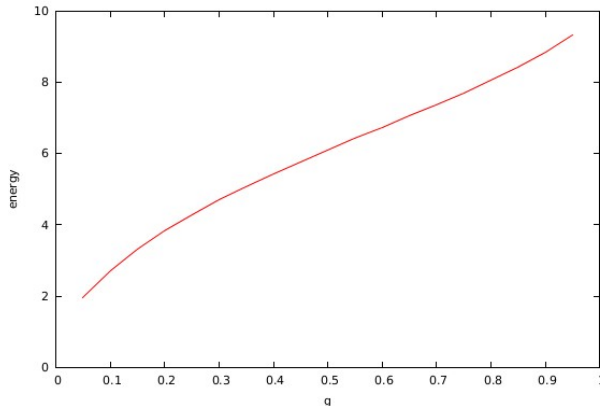


Figure 4: The energy of the static Skyrmion as a function of the parameter  $g$ .

Computations for other values of this parameter have also been performed, and the qualitative features remain unchanged. Our numerical grids have a lattice spacing  $\Delta x = \Delta y = 0.08$  and the smallest grids used contain  $300 \times 150$  lattice points in the  $(x, y)$  plane, with larger grids used for simulations involving multi-Skyrmions. Spatial derivatives are approximated using a fourth-order accurate finite difference scheme. The Dirichlet and Neumann boundary conditions, defined above at spatial infinity, are applied at the boundary of the numerical grid.

In Figure 3 we present the result of a numerical computation of the static Skyrmion by plotting the energy density (the integrand in (2.2)) in the left image and the topological charge density (the integrand in (2.4)) in the right image. The domain wall is not visible in the plot of the topological charge density because this vanishes for a domain wall. This plot therefore highlights only the Skyrmion.

The domain wall is clearly evident in the energy density plot, with the Skyrmion located on the wall and producing a peak in the energy density. As  $g \rightarrow 0$  the width of the domain wall tends to a non-zero value proportional to  $1/m$ . However, for small  $g$  the width of the kink is much larger than this, as it scales like  $1/(m\sqrt{g})$ . The Skyrmion therefore appears as a structure that is stretched in the direction of the domain wall, although this stretching effect is reduced as  $g$  increases towards 1.

The energy of a domain wall is infinite but the additional contribution due to the presence of a Skyrmion is finite. We may therefore define the energy of a Skyrmion as the difference between the energies of the domain wall Skyrmion and the pure domain wall solution. In Figure 4 we plot the static Skyrmion energy as a function of the parameter  $g$ . This energy

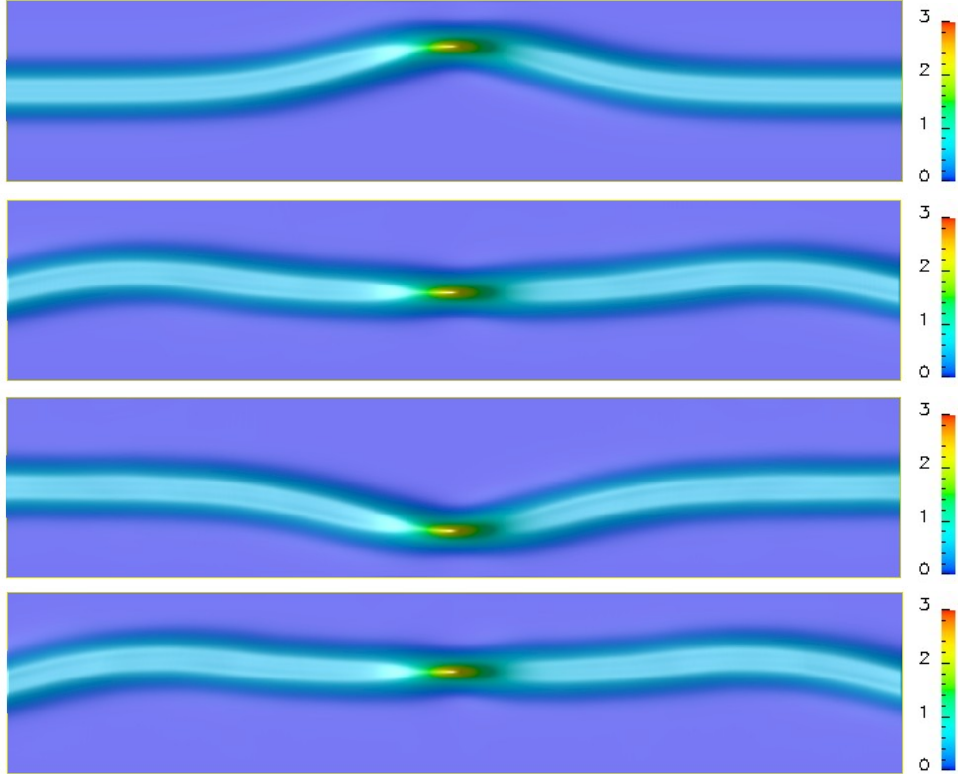


Figure 5: Energy density plots at increasing times (from top to bottom  $t = 0, 25, 60, 100$ ) for a perturbed domain wall Skyrmion.

increases with  $g$  and is approximately linear for most of the range of  $g$ .

### 3 Skyrmion dynamics

To investigate Skyrmion dynamics we numerically solve the (2+1)-dimensional nonlinear wave equation that follows from the variation of the Lagrangian density (2.1). The spatial aspects of the algorithm are as described in the previous section on static Skyrmons, and the time evolution is simulated using a fourth-order Runge-Kutta method with a timestep  $\Delta t = 0.02$ .

To test the stability of the Skyrmion we have examined the evolution of a number of initial conditions in which a perturbation is applied to the static solution. A typical example is presented in Figure 5, in which a wiggle is introduced into the domain wall. The initial wiggle results in an oscillation of the domain wall, but the Skyrmion remains intact on the wall during this motion. The amplitude of the oscillation slowly decreases as the wall radiates. This radiation can escape from the system because of the Neumann boundary condition, and eventually the static domain wall Skyrmion is recovered. This, and similar results, provide strong evidence for the stability of the domain wall Skyrmion.



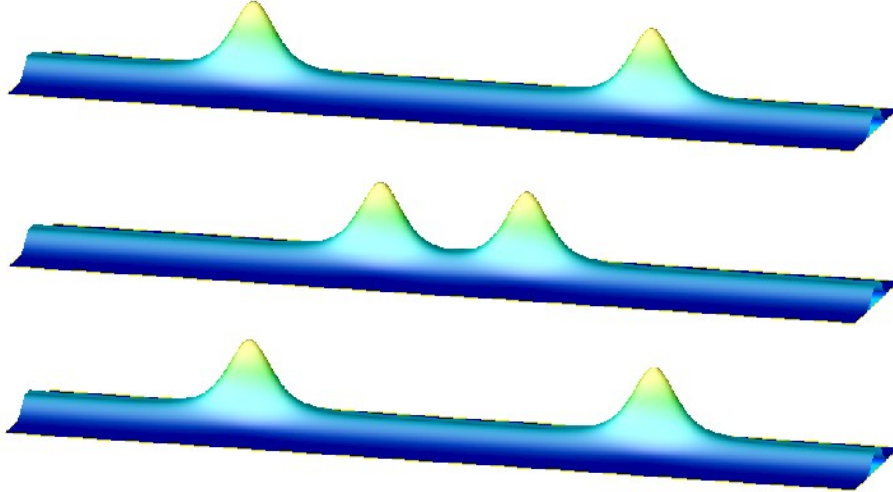


Figure 6: Energy density plots at increasing times (from top to bottom  $t = 0, 54, 108$ ) for the scattering of two Skyrmions. Each Skyrmion has an initial velocity  $v = 0.2$  towards the other Skyrmion.

Viewing the domain wall Skyrmion as a sine-Gordon kink on a domain wall suggests that two Skyrmions are repulsive, since there is a repulsive force between two sine-Gordon kinks [12]. This is indeed the case, as verified by evolving an initial condition that contains two well-separated Skyrmions on the domain wall. Furthermore, a comparison between the dynamics of two domain wall Skyrmions and two sine-Gordon kinks reveals a good agreement for scattering at low speeds. An example scattering event is shown in Figure 6, in which each Skyrmion is Lorentz boosted with an initial velocity  $v = 0.2$  towards the other Skyrmion. The Skyrmions approach to a minimal separation and bounce back, due to the repulsive force, in an almost elastic collision that generates very little radiation.

We now compare this Skyrmion scattering with kink scattering in the integrable sine-Gordon theory (2.9). In Figure 7 the red curves in the images on the left show  $-n_2$  along the line  $y = 0$  (ie. along the domain wall) at increasing times during this scattering. The blue curves display  $-\cos \varphi$  for the corresponding exact sine-Gordon 2-kink scattering solution

$$\varphi = 4 \tan^{-1} \left( \frac{v \sinh(\gamma m \sqrt{\frac{g}{2}} x)}{\cosh(\gamma m \sqrt{\frac{g}{2}} v(t - t_0))} \right), \quad (3.1)$$

where  $\gamma = 1/\sqrt{1 - v^2}$ . Here  $t_0$  is a constant that determines the kink separation at time  $t = 0$ , and is fixed to match with the initial conditions of the field theory simulation.

The images on the left in Figure 7 reveal a good agreement between the Skyrmions in the field theory simulations and the kinks in the effective theory. The main difference is that the minimal separation between the Skyrmions is slightly less than the minimal separation between the kinks. The Skyrmions get a little closer together than the kinks because as they squeeze together they begin to explore the extra dimension. This results in a slight increase in the time delay before the Skyrmions bounce back. This is evident in the images at later

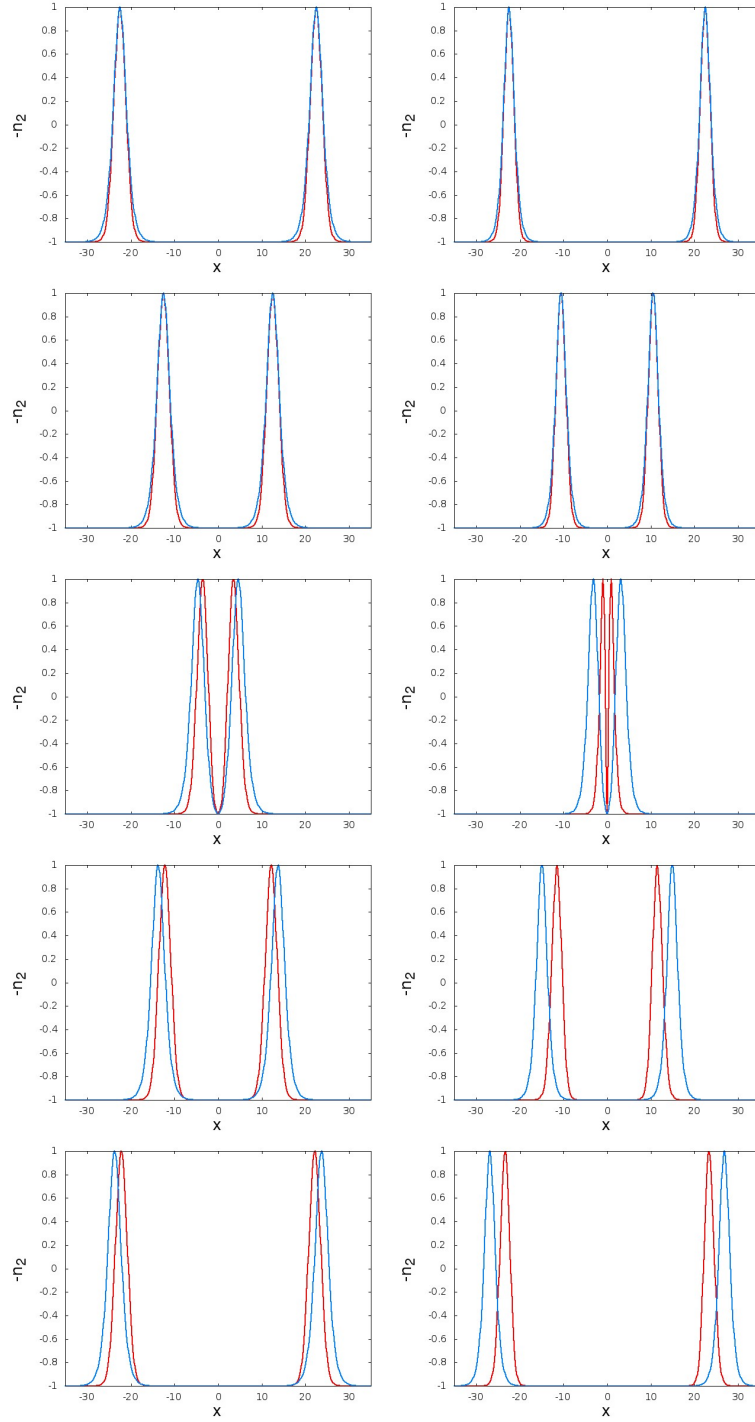


Figure 7: The field  $-n_2$  (red curves) along the domain wall  $y = 0$  at increasing times (from top to bottom) for an initial configuration in which each Skyrmion has an initial velocity  $v$  towards the other Skyrmion. The associated sine-Gordon approximation is also shown (blue curves). The images on the left are for  $v = 0.2$  and times  $t = 0, 50, 100, 150, 200$ . The images on the right are for  $v = 0.6$  and times  $t = 0, 20, 40, 60, 80$ .

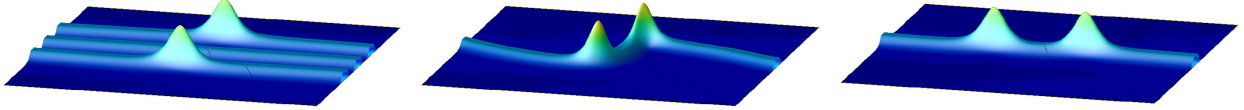


Figure 8: Energy density plots at increasing times for the evolution (with damping) of two Skyrmions that are initially on different domain walls. In the left image ( $t = 0$ ) the two Skyrmions have initial positions  $(-1, -7)$  and  $(1, 7)$ . There are walls along  $y = \pm 7$  and an anti-wall along  $y = 0$ . All time derivatives are initially zero. In the middle image ( $t = 60$ ) the Skyrmions have survived the wall anti-wall annihilation process. In the right image ( $t = 135$ ) the Skyrmions are moving apart along the remaining straight wall.

times, where the red curves are slightly inside the blue curves. This effect becomes more pronounced as the initial speed  $v$  increases, as this provides more energy to explore the extra dimension. The images on the right in Figure 7 show a similar comparison for a scattering at the increased speed  $v = 0.6$ . The closer approach of the Skyrmions is now more apparent, as is the increased time delay.

The analogue of other phenomena that appear in the sine-Gordon theory, for example breathers, could also be investigated for domain wall Skyrmions. However, we now turn to Skyrmion scattering events that are beyond the realm of the effective (1+1)-dimensional theory, by considering a fully planar process in which two Skyrmions are initially on different domain walls.

The vacuum structure of the theory is not compatible with a field configuration in which two domain walls are placed next to each other. However, a field configuration in which walls and anti-walls alternate is allowed. An anti-wall is obtained from a wall by the replacement  $n_3 \mapsto -n_3$ . The simplest arrangement that allows Skyrmions to be placed on different walls involves an initial setup in which an anti-wall is sandwiched between two walls that each contain a Skyrmion.

An example of such an initial configuration is displayed in the left image in Figure 8, in which there are walls along  $y = \pm 7$  and an anti-wall along  $y = 0$ . There is a Skyrmion on each wall, with initial Skyrmion positions given by  $(-1, -7)$  and  $(1, 7)$ . All initial time derivatives are set to zero, so the kinetic energy vanishes at the start of the simulation. It is important that there is an excess of walls over anti-walls, since a wall and an anti-wall will generally annihilate. Obviously, a wall is required in the final state if domain wall Skyrmions are to be present. As the wall anti-wall annihilation process will generate a large amount of kinetic energy, a damping term is included in the dynamics to dissipate some of this kinetic energy. This aids the visualization of the Skyrmions (as otherwise this contribution to the energy density can swamp that of the Skyrmions) and also reduces any numerical difficulties associated with this radiation reflecting from the boundary of the grid.

The attraction between a wall and an anti-wall generates a motion in which the two walls move towards the anti-wall. However, the fact that the Skyrmion on the wall along  $y = 7$  has a positive  $x$  coordinate results in a slightly reduced speed of the wall at positive values of  $x$  compared to the equivalent negative values. A similar effect takes place for the other wall,

but as the offset is in the reverse direction then the opposite side of the wall is the portion with a slightly reduced speed. The net result is that for positive  $x$  the anti-wall annihilates with the wall which initially has a negative value of  $y$ , whereas for negative  $x$  the anti-wall annihilates with the wall with an initial positive value of  $y$ . The outcome is that two half-walls survive that are joined by Skyrmions at their ends (see the middle image in Figure 8). The Skyrmions survive the process in which the two half-walls straighten into a single wall, and subsequently the Skyrmions move apart along the remaining straight wall, due to their repulsive interaction (see the right image in Figure 8). The fact that the Skyrmions survive this complicated and quite violent process is further evidence in support of their stability.

We have performed similar simulations with other choices of initial positions and we have also varied the strength of the damping term, but the qualitative features remain unchanged. If no initial offset is introduced into the  $x$  components of the Skyrmion positions then there is nothing to break the symmetry of the configuration, and hence the Skyrmions no longer separate along the  $x$ -axis. However, this highly symmetric situation is unstable and even tiny numerical effects can be enough to break the symmetry and yield the same kind of scattering as just described.

## 4 Conclusion

In this paper we have studied planar Skyrmions in a relativistic theory without a Skyrme term. In particular, we have presented the first results on the dynamics of such domain wall Skyrmions. We have investigated both Skyrmion stability and multi-Skyrmion scattering. The latter have been compared to kink scattering in the sine-Gordon model, which is an effective (1+1)-dimensional theory applicable to evolution in which all Skyrmions remain on the same wall. More exotic phenomena have also been presented, in which Skyrmions on different domain walls can emerge on the same wall. These examples demonstrate that the dynamics of domain wall Skyrmions can be very complex and quite different from the usual dynamics found for Skyrmions in theories with a Skyrme term.

For numerical simplicity, we have considered a planar theory in this work, but we expect similar results to apply in related (3+1)-dimensional models. Examples of suitable (3+1)-dimensional theories are discussed in [8]. It might be of interest to extend the kind of numerical work described in this paper to these higher-dimensional theories.

Obtaining physical theories that include a Skyrme term is often problematic, as higher-derivative terms tend not to arise naturally. In contrast, domain walls are ubiquitous in many areas of cosmology, high-energy physics and condensed matter physics. It is therefore of considerable interest to determine the properties of domain wall Skyrmions as there are a wide range of opportunities for potential applications. Some of these are currently under investigation.

## Acknowledgements

PJ is supported by an STFC studentship. PMS acknowledges funding from EPSRC under grant EP/K003453/1 and STFC under grant ST/J000426/1.

## References

- [1] T. H. R. Skyrme, A nonlinear field theory, *Proc. R. Soc. Lond.* **A260**, 127 (1961); A unified field theory of mesons and baryons, *Nucl. Phys.* **31**, 556 (1962).
- [2] G. H. Derrick, Comments on nonlinear wave equations as models for elementary particles, *J. Math. Phys.* **5**, 1252 (1964).
- [3] B. M. A. G. Piette, B. J. Schroers and W. J. Zakrzewski, Multisolitons in a two-dimensional Skyrme model, *Z. Phys.* **C65**, 165 (1995).
- [4] S. L. Sondhi, A. Karlhede, S. A. Kivelson and E. H. Rezayi, Skyrmions and the crossover from the integer to fractional quantum Hall effect at small Zeeman energies, *Phys. Rev.* **B47**, 16419 (1993).
- [5] X. Z. Yu, Y. Onose, N. Kanazawa, J. H. Park, J. H. Han, Y. Matsui, N. Nagaosa and Y. Tokura, Real-space observation of a two-dimensional skyrmion crystal, *Nature* **465**, 901 (2010).
- [6] N. S. Manton and P. M. Sutcliffe, *Topological Solitons*, Cambridge University Press (2004).
- [7] *The Multifaceted Skyrmion*, Eds. G. E. Brown and M. Rho, World Scientific Publishing (2010).
- [8] M. Nitta, Josephson vortices and the Atiyah-Manton construction, *Phys. Rev.* **D86**, 125004 (2012); Matryoshka Skyrmions, *Nucl. Phys.* **B872**, 62 (2013); Correspondence between Skyrmions in 2+1 and 3+1 dimensions, *Phys. Rev.* **D87**, 025013 (2013).
- [9] M. Kobayashi and M. Nitta, Jewels on a wall ring, *Phys. Rev.* **D87**, 085003 (2013).
- [10] R. A. Leese, M. Peyrard and W. J. Zakrzewski, Soliton stability in the  $O(3)$   $\sigma$ -model in (2+1) dimensions, *Nonlinearity* **3**, 387 (1990).
- [11] T. Weidig, The baby Skyrme models and their multi-skyrmions, *Nonlinearity* **12**, 1489 (1999).
- [12] J. K. Perring and T. H. R. Skyrme, A model unified field equation, *Nucl. Phys.* **31**, 550 (1962).